Article

Effects of Packing Structure on the Optoelectronic and Charge Transport Properties in Poly(9,9-di-*n*-octylfluorene-*alt*-benzothiadiazole)

Carrie L. Donley, Jana Zaumseil, Jens W. Andreasen, Martin M. Nielsen, Henning Sirringhaus, Richard H. Friend, and Ji-Seon Kim

J. Am. Chem. Soc., **2005**, 127 (37), 12890-12899• DOI: 10.1021/ja051891j • Publication Date (Web): 25 August 2005

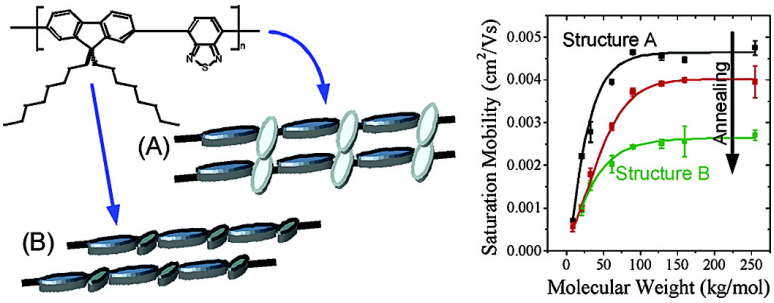

More About This Article

Additional resources and features associated with this article are available within the HTML version:

- Supporting Information
- Links to the 28 articles that cite this article, as of the time of this article download
- Access to high resolution figures
- Links to articles and content related to this article
- Copyright permission to reproduce figures and/or text from this article

View the Full Text HTML

J|A|C|S
ARTICLES
Published on Web 08/25/2005

Effects of Packing Structure on the Optoelectronic and Charge Transport Properties in Poly(9,9-di-*n*-octylfluorene-*alt*-benzothiadiazole)

Carrie L. Donley,*,† Jana Zaumseil,† Jens W. Andreasen,§ Martin M. Nielsen,§ Henning Sirringhaus,† Richard H. Friend,† and Ji-Seon Kim*,†

Contribution from the Department of Physics, Cavendish Laboratory, University of Cambridge, Cambridge CB3 0HE, England, and Danish Polymer Centre, Risø National Laboratory, DK-4000 Roskilde, Denmark

Received March 24, 2005; E-mail: cld37@cam.ac.uk; jsk20@cam.ac.uk

Abstract: Spin-coated poly(9,9-di-*n*-octylfluorene-*alt*-benzothiadiazole) (F8BT) films of different molecular weights ($M_n = 9-255$ kg/mol), both in the pristine and annealed state, were studied in an effort to elucidate changes in the polymer packing structure and the effects this structure has on the optoelectronic and charge transport properties of these films. A model based on quantum chemical calculations, wide-angle X-ray scattering, atomic force microscopy, Raman spectroscopy, photoluminescence, and electron mobility measurements was developed to describe the restructuring of the polymer film as a function of polymer chain length and annealing. In pristine high molecular weight films, the polymer chains exhibit a significant torsion angle between the F8 and BT units, and the BT units in neighboring chains are close to one another. Annealing films to sufficiently high transition temperatures allows the polymers to adopt a lower energy configuration in which the BT units in one polymer chain are adjacent to F8 units in a neighboring chain ("alternating structure"), and the torsion angle between F8 and BT units is reduced. This restructuring, dictated by the strong dipole on the BT unit, subsequently affects the efficiencies of interchain electron transfer and exciton migration. Films exhibiting the alternating structure show significantly lower electron mobilities than those of the pristine high molecular weight films, due to a decrease in the efficiency of interchain electron transport in this structure. In addition, interchain exciton migration to low energy weakly emissive states is also reduced for these alternating structure films, as observed in their photoluminescence spectra and efficiencies.

Introduction

Since the first reports of electroluminescence in conjugated polymers,[1] conjugated polymers with a variety of structures have been investigated for use in light-emitting diodes, photovoltaic cells, and field effect transistors. Polyfluorenes are one class of conjugated polymers receiving attention lately,[2,3] due to the ease of spin coating or drop casting solutions of these polymers substituted with solubilizing side chains. Variations in the deposition conditions, such as the solvent or temperature, allow different packing structures in homopolymer films and different degrees of phase separation in blend films.[4−8] Additionally, many fluorene copolymers have also been investigated in an effort to tune the optical properties of these versatile materials.

Poly(9,9-di-*n*-octylfluorene-*alt*-benzothiadiazole) (F8BT, chemical structure in Figure 1) is a fluorene copolymer with alternating F8 and BT units that has been extensively used in blends with other fluorene copolymers, such as poly(9,9′-di-*n*-octylfluorene-*alt*-*N*-(4-butylphenyl)diphenylamine) (TFB) and poly(9,9′-di-*n*-octylfluorene-*alt*-bis-*N*-*N*′-(4-butylphenyl)bis-*N*,*N*′-phenyl-1,4-phenylenediamine) (PFB), for efficient light-emitting diodes and photovoltaic cells, respectively.[4−11] In both of these cases, F8BT plays the role of the electron transport agent; however, the mechanisms for intra- and interchain charge transport in these polymers are not well understood. Specifically, correlations between particular polymer packing structures and charge transfer have not been extensively studied. Polymer packing structures are also expected to affect the optical properties of

† University of Cambridge.
§ Risø National Laboratory.

(1) Burroughes, J. H.; Bradley, D. D. C.; Brown, A. R.; Marks, R. N.; Mackay, K.; Friend, R. H.; Burns, P. L.; Holmes, A. B. *Nature* **1990**, *347*, 539.
(2) Neher, D. *Macromol. Rapid Commun.* **2001**, *22*, 1365.
(3) Scherf, U.; List, E. J. W. *Adv. Mater.* **2002**, *14*, 477.
(4) Arias, A. C.; Corcoran, N.; Banach, M. J.; Friend, R. H.; MacKenzie, J. D.; Huck, W. T. S. *Appl. Phys. Lett.* **2002**, *80*, 1695.
(5) Snaith, H. J.; Arias, A. C.; Morteani, A. C.; Silva, C.; Friend, R. H. *Nano Lett.* **2002**, *2*, 1353.
(6) Corcoran, N.; Arias, A. C.; Kim, J. S.; MacKenzie, J. D.; Friend, R. H. *Appl. Phys. Lett.* **2003**, *82*, 299.
(7) Halls, J. J. M.; Arias, A. C.; MacKenzie, J. D.; Wu, W.; Inbasekaran, M.; Woo, E. P.; Friend, R. H. *Adv. Mater.* **2000**, *12*, 498.
(8) Kim, J.-S.; Ho, P. K. H.; Murphy, C. E.; Friend, R. H. *Macromolecules* **2004**, *37*, 2861.
(9) Seeley, A. J. A. B.; Friend, R. H.; Kim, J.-S.; Burroughes, J. H. *J. Appl. Phys.* **2004**, *96*, 7643.
(10) Redecker, M.; Bradley, D. D. C.; Inbasekaran, M.; Wu, W. W.; Woo, E. P. *Adv. Mater.* **1999**, *11*, 241.
(11) Morteani, A. C.; Dhoot, A. S.; Kim, J.-S.; Silva, C.; Greenham, N. C.; Murphy, C. E.; Moons, E.; Cina, S.; Burroughes, J. H.; Friend, R. H. *Adv. Mater.* **2003**, *15*, 1708.

10.1021/ja051891j CCC: $30.25

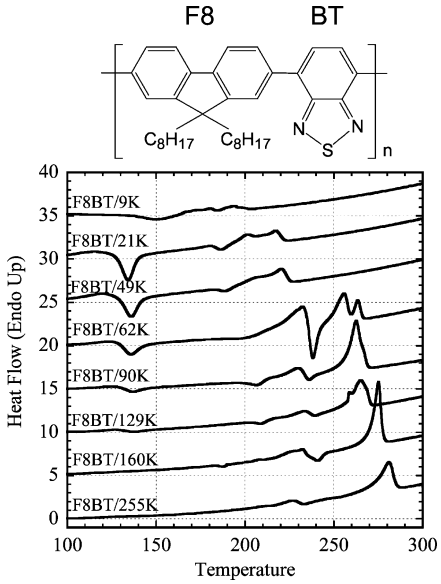

Figure 1. (Top) The chemical structure of F8BT. (Bottom) Differential scanning calorimetry data for all of the molecular weights investigated. Only the second heating scans are shown. These data were used to determine the transition temperatures and establish annealing procedures (Table 1).

these molecules, especially the formation of interchain species, such as aggregate and excimer states.

In addition, many structural parameters can affect the optoelectronic and charge transport properties in conjugated polymer thin films. The orientation of the polymer chains with respect to the electrodes in a device structure and the degree of crystallinity can play a crucial role in charge carrier mobilities, for example. The interchain π-spacing may affect the rate of interchain charge transfer, the torsion angle between neighboring units within a single polymer chain will affect the planarity and effective conjugation length of the chain, and interchain polymer packing structures can significantly effect both charge and energy transport. All of these structural issues will be addressed in this paper for F8BT films.

Quantum chemical calculations of the lowest unoccupied molecular orbital (LUMO) levels of the BT and F8 units have revealed that the LUMO of the BT unit lies 1.56 eV lower than the LUMO of the fluorene unit, resulting in a strong localization of electrons on the BT unit in the LUMO of F8BT.[12] In this paper, the optoelectronic and charge transport properties that result from this strong electron localization are investigated in molecules of F8BT with systematically varied molecular weights (M_n) from 9 to 255 kg/mol. We use wide-angle X-ray scattering, ellipsometry, Raman spectroscopy, and atomic force microscopy as probes of the structural changes that occur within pristine films of various molecular weights and the additional reorganization that occurs after annealing. We show that the various polymer packing structures influence the optoelectronic properties of these thin F8BT films, as well as the electron carrier mobilities measured in field effect transistors.

Experimental Section

F8BT materials ranging in molecular weight (M_n) from 9 to 255 kg/mol (Table 1) were received from Cambridge Display Technology Ltd. and used without further purification. The materials examined in this study involve a larger range of F8BT molecular weights than previously available.[13,14] Molecular weights were determined by gel permeation chromatography in comparison to polystyrene standards. F8BT films for all molecular weights were spin cast from *o*-xylene solutions ranging in concentration from 1 to 1.8% (w/v) to produce films approximately 100 nm thick without significant variation in the spin conditions. Films were spun on spectrosil (quartz) or silicon substrates that had been cleaned by successive 15 min sonications in acetone and 2-propanol followed by cleaning in an oxygen plasma for 10 min (250 W).

Table 1. Properties and Annealing Temperatures of the Polymers Examined

sample	degree of polymerization	M_n	polydispersity	annealing temperature (above T_g)	annealing temperature (above T_m)
F8BT/9K	5.7	9 kg/mol	3.45	155 °C	215 °C
F8BT/21K	13.4	21 kg/mol	3.35	155 °C	235 °C
F8BT/49K	31.5	49 kg/mol	1.82	155 °C	240 °C
F8BT/62K	39.6	62 kg/mol	2.73	155 °C	280 °C
F8BT/90K	57.5	90 kg/mol	1.99	155 °C	280 °C
F8BT/129K	82.4	129 kg/mol	1.77	155 °C	280 °C
F8BT/160K	102.2	160 kg/mol	1.75	155 °C	290 °C
F8BT/255K	162.8	255 kg/mol	1.55	155 °C	300 °C

A Perkin-Elmer Pyris 1 differential scanning calorimeter (DSC) was used to determine the transition temperatures of the F8BT samples. DSC experiments were carried out in three stages. The first heating stage was from 30 to 300 °C, followed by cooling back to 30 °C, and a second heating cycle to 300 °C, all at a rate of 20 °C/min. Thermal transitions were determined by the first cooling and the second heating scans, and they defined the annealing conditions for thin films (Table 1). For the annealing studies, samples were heated to the appropriate temperature in a nitrogen environment for 1 h and then either slowly cooled or quickly quenched (hot samples were placed on a piece of metal at room temperature).

Samples for wide-angle X-ray scattering were prepared on both silicon and thin BCB/silicon substrates (described below). The wide-angle X-ray scattering was measured in a grazing incidence geometry (GIWAXS) at the Danish Polymer Centre X-ray Facility, Risø. The Cu Kα,β radiation is generated by a rotating anode operating at 10 kW and is focused, collimated, and filtered (only Cu Kα is selected) by a multilayer X-ray mirror. Scattering from the sample substrate is suppressed, except from the topmost layers, by setting the sample surface at an angle to the X-ray beam smaller than the critical angle for total reflection for the sample substrate.[15] In this manner, scattering measurements of nanometer thin films are feasible. The scattered signal was recorded on photo stimulable image plates.

AFM images were obtained with a Digital Instruments/Veeco Dimension 3100 atomic force microscope (AFM) operated in the tapping mode.

A Renishaw 2000 Raman microscope was used to collect Raman spectra. Samples were excited with a HeNe laser (633 nm) focused on the sample with a 100X microscope objective, and the scattered Raman signal was collected through the same objective and detected by a CCD camera. A 20 s integration time was used, and the signal was summed over 10 scans in the extended scan mode. After irradiation, the samples were visually inspected through the microscope, but no signs of laser damage to the sample were observed.

Absorption spectra for solutions and thin films were acquired with a Hewlett-Packard 8453 diode array spectrometer. Both photolumi-

(12) Cornil, J.; Gueli, I.; Dkhissi, A.; Sancho-Garcia, J. C.; Hennebicq, E.; Calbert, J. P.; Lemaur, V.; Beljonne, D.; Bredas, J. L. *J. Chem. Phys.* **2003**, *118*, 6615.

(13) Banach, M. J.; Friend, R. H.; Sirringhaus, H. *Macromolecules* **2003**, *36*, 2838.

(14) Snaith, H. J.; Friend, R. H. *Thin Solid Films* **2004**, *451*−*52*, 567.

(15) Als-Nielsen, J.; McMorrow, D. Refraction and Reflection from Interfaces. In *Elements of Modern X-ray Physics*; John Wiley & Sons: Chichester, U.K., 2000; p 61.

nescence (PL) spectra and efficiencies were measured at room temperature in a nitrogen-purged integrating sphere with excitation from an argon ion laser at 457 nm for thin films and a helium cadmium laser at 325 nm for solutions. PL efficiencies were calculated as described by de Mello and co-workers.[16]

Electron mobilities were determined using n-channel field-effect transistors with F8BT as the active semiconducting layer. A highly doped silicon wafer acted as a substrate and bottom gate. The first part of the gate dielectric was formed by 300 nm thick thermally grown SiO_2. A second dielectric layer was added by spinning a benzocyclobutene (BCB) monomer (Cyclotene from Dow Chemical Company) from a 6 wt % mesitylene solution and cross-linking at 290 °C.[17] This 50−60 nm buffer layer ($\epsilon = 2.65$) eliminates electron trapping at the dielectric−semiconductor interface, which normally prevents observation of electron transport in F8BT.[18] The total capacitance of this bilayer dielectric was measured to be 9 nF/cm^2. Spinning F8BT onto the dielectric from anhydrous xylene solutions led to 50−70 nm thin films, which were annealed to various temperatures as described below for 1 h and slowly cooled. Interdigitated source and drain electrodes were then evaporated through a shadow mask, forming a transistor with a channel length of 200 μm and a channel width of 10 cm. Deposition of a 100 nm thick silicon monoxide encapsulation layer completed the device. All processing steps were carried out under the exclusion of oxygen and water. Transistor characteristics were measured using an Agilent 4155C semiconductor parameter analyzer. The electron mobility in the saturation regime was calculated according to standard transistor equations.[19] Mobilities calculated using the linear regime of device operation were typically 5−10% smaller than those calculated in the saturation regime.

Results

Differential Scanning Calorimetry (DSC). DSC was performed to determine the transition temperatures of the F8BT molecules under investigation, and the second heating scans are shown in Figure 1. Cooling scans did not exhibit major transitions; however, many did show a weak transition near the first transition in the heating cycle. Most of the molecules show a transition near 135−140 °C, which has been previously assigned to a transition from the glassy to rubbery state along with some crystallization due to the exothermic nature of the shift.[13] The second transition is an exothermic transition due to additional crystallization of the polymers ranging in temperature from 185 to 230 °C as the molecular weight of the polymers increases. Finally, the polymers exhibit a final endothermic transition due to melting (T_m) into a liquid crystalline phase that ranges from 195 to 280 °C. These temperatures have been used to define annealing temperatures for the experiments that follow. Samples were annealed to temperatures either just above the glass transition temperature (T_g) or just above the melting temperature (T_m), as described in Table 1, and then either slowly cooled (SC) or quickly quenched (Q).

Wide-Angle X-ray Scattering. Wide-angle X-ray scattering (WAXS) data were obtained for films of F8BT/255K and F8BT/9K (Figure 2). These data clearly show samples with different degrees of crystallinity and various unit cell parameters; however, all WAXS images show the characteristic spacing of 4.18 Å (indicated by the (001) and (004) rings in Figure 2a),

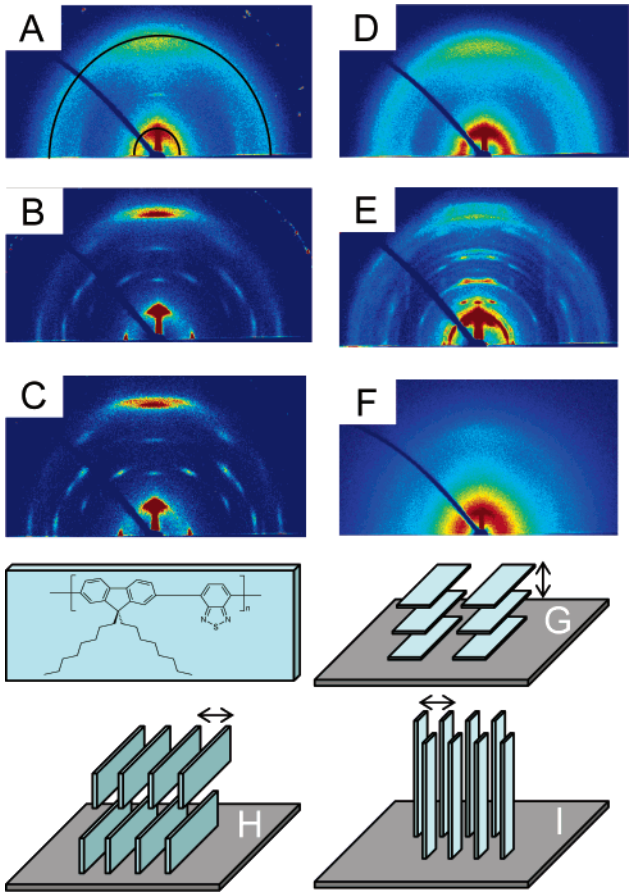

Figure 2. WAXS data for F8BT/255K (A−C) and F8BT/9K (D−F). (A and D) Pristine, (B and E) annealed to T_g and slowly cooled, and (C and F) annealed to T_m and slowly cooled. The inner and outer rings in (A) correspond to the (001) and (004) reflections, respectively. Possible orientations of the polymers with respect to the substrate are shown in (G−I), with the π-stacking direction indicated by arrows. Analysis of the WAXS and ellipsometry data indicates that in all samples the predominant orientation is similar to that in (G).

corresponding to the π-stacking between polymers. Similar spacings are also observed in other conjugated semiconducting polymers,[20−22] indicating that this distance may be critical for efficient charge transport. The intensity of the (001) and (004) rings in pristine films is not uniformly distributed. The F8BT/255K film shows slightly more intensity in the vertical direction (normal to the substrate), indicating that the polymer backbone is oriented in the plane of the substrate and the π-stacking spacing is normal to the substrate (orientation illustrated in Figure 2g). The slightly more uniform intensity distribution of the (001) and (004) rings in the pristine F8BT/9K sample indicates a more random orientation of the polymer chains. Ellipsometry data have indicated a preferential orientation of the polymer backbones in the plane of the substrate for all F8BT samples; however, the larger molecular weight samples show a higher dichroism in the extinction coefficient, k ($k_{in-plane}/k_{out-of-plane} = 5.8$ for pristine F8BT/255K and 3.4 for pristine F8BT/9K at 460 nm). This ellipsometry data indicates that the

(16) deMello, J. C.; Wittmann, H. F.; Friend, R. H. *Adv. Mater.* **1997**, *9*, 230.
(17) Chua, L. L.; Ho, P. K. H.; Sirringhaus, H.; Friend, R. H. *Appl. Phys. Lett.* **2003**, *84*, 3400.
(18) Chua, L. L.; Chang, J.-F.; Zaumseil, J.; Ou, E. C. W.; Ho, P. K. H.; Sirringhaus, H.; Friend, R. H. *Nature* **2005**, *434*, 194.
(19) Dimitrakopoulos, C. D.; Malenfant, P. R. L. *Adv. Mater.* **2002**, *14*, 99.
(20) Sirringhaus, H.; Brown, P. J.; Friend, R. H.; Nielsen, M. M.; Bechgaare, K.; Langeveld-Voss, B. M. W.; Spiering, A. J. H.; Janssen, R. A. J.; Meijer, E. W.; de Leeuw, D. M. *Nature* **1999**, *401*, 685.
(21) Bao, Z. N.; Lovinger, A. J. *Chem. Mater.* **1999**, *11*, 2607.
(22) Cornil, J.; Beljonne, D.; Calbert, J. P.; Bredas, J. L. *Adv. Mater.* **2001**, *13*, 1053.

pristine F8BT/9K samples contain a larger percentage of polymer chains oriented vertically, as in Figure 2i, and thus the intensity observed in the horizontal (in-plane) direction in the WAXS data is most likely due to polymer chains oriented in this direction, and not as shown in Figure 2h.

Upon annealing the F8BT/255K sample, clear texture appears in the WAXS image, indicating the preferential orientation of the unit cell (a = 14.65 Å, b = 5.3 Å, and c = 16.7 Å) with respect to the substrate. We consider that the in-plane a-axis lies along the backbone of the polymer chain as this distance is approximately that of one F8−BT repeat unit. The in-plane b-axis is thought to be the interchain spacing, which is rather small considering the alkyl chains must pack in this direction. The long out-of-plane c-axis is thought to be 4 times the π-stacking spacing (4.18 Å). The $a-b$ face of this monoclinic unit cell is parallel to the substrate surface with the c-axis oriented 98° from the $a-b$ plane. The reflections in the sample annealed to T_m are sharper than those in the T_g sample, indicating larger crystalline domains. WAXS data of F8BT/255 K annealed to T_m on a BCB/silicon substrate showed the same crystalline structure as that in Figure 2c on a silicon substrate, which will be relevant to the discussion of the n-type mobilities described below.

Annealing F8BT/9K to T_g results in a structure that is markedly different from that in F8BT/255K. Some portion of the film retains the disordered structure present in the pristine film. Another portion displays the unit cell described above, although with very weak reflections, and an additional unit cell with larger dimensions is also present. Annealing above T_m results in a scattering pattern similar to that for pristine films.

A clear description of the arrangement of these polymer chains in the unit cell has not yet been achieved, even for annealed films of F8BT/255K; however, the results of the experiments described below clearly indicate that this structural change is significant, and that the more ordered structure found in annealed F8BT films is not always ideal. For this reason, we have relied on other techniques, such as Raman spectroscopy and photoluminescence spectroscopy, to elucidate more detailed information about the local packing structures of these polymer chains.

Atomic Force Microscopy (AFM). AFM images of pristine F8BT films were very similar, with only a small but systematic increase in the RMS roughness of the samples with decreasing molecular weight (from 0.66 nm for F8BT/255K to 1.0 nm for F8BT/9K, on the 5 μm scale). Upon annealing, the surface roughness increased for all annealing conditions. Figure 3 illustrates the structural changes that occur in the highest and lowest molecular weight films.

The low molecular weight polymer films exhibit a different temperature dependence as compared to that of the high molecular weight films. For these films, lower annealing temperatures are sufficient to induce significant morphological changes. F8BT/9K films showed exceptional reorganization after annealing to T_g, as shown in Figure 3g,h, changes similar to those observed in some other polyfluorene films.[23] The F8BT film now exhibits strands of material that run parallel to each other until coming upon another area of material where they may split apart or change directions (most clearly observed at the bottom of Figure 3g), a very different morphology from

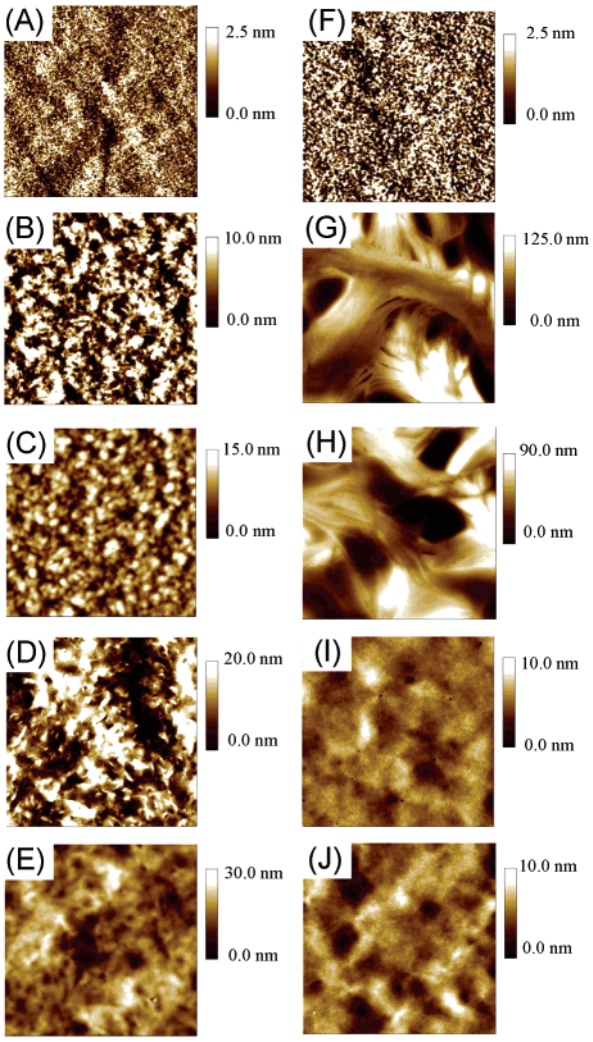

Figure 3. AFM images (5 μm × 5 μm) of pristine and annealed F8BT thin films. Images on the left side (A−E) are of F8BT/255K, while those on the right side (F−J) are of F8BT/9K. (A and F) pristine films, (B and G) T_g, slowly cooled, (C and H) T_g, quenched, (D and I) T_m, slowly cooled, and (E and J) T_m, quenched.

that observed in the rather amorphous-looking pristine films. Annealing to above T_m, however, does not have the same effect on these films; AFM images exhibited very small RMS roughnesses (RMS roughness ∼ 1.8 nm), and no surface structure was evident. These images seem to compliment the WAXS data for this sample; however, F8BT/9K samples annealed to T_g and T_m showed the same amount of birefringence under crossed polarizers, indicating a significant degree of order in annealed films. The ordering (or lack thereof) in this sample is not well understood at this time.

The cooling conditions were found to affect the surface roughness of the larger molecular weight films annealed to T_m. Slowly cooled samples showed higher RMS roughness values (8 nm for F8BT/255K) as compared to those that were quenched back to room temperature (5 nm for F8BT/255K). Slow cooling is expected to allow the polymers to form larger crystalline domains and lead to the larger surface roughness values.

Raman Spectroscopy. Raman spectra obtained here are simpler than infrared (IR) spectra since vibrational modes that are coupled to the conjugated backbone (chromophore) are strongly enhanced due to a stronger polarization of electrons

(23) Teetsov, J. A.; Vanden Bout, D. A. *J. Am. Chem. Soc.* **2001**, *123*, 3605.

along the conjugated backbone.[24] Raman spectra of pristine F8BT films were similar to those reported elsewhere,[8,25] and the full spectrum is not shown here. For all of the thin film spectra, no changes were observed in the two main peaks associated with the polymer backbone at 1545 and 1608 cm^{-1} (ring stretching modes for the BT and F8 units, respectively[8,25,26]), and thus, one of these peaks (1545 cm^{-1}) was chosen for normalization purposes for all of the Raman spectra. The only differences in the Raman spectra of pristine films as a function of molecular weight were observed in the energy region shown in Figure 4a. The relative intensity of the peak at 1358 cm^{-1} decreases with decreasing molecular weight, and thus its intensity will be the main focus of these studies.

After annealing, the intensities of many peaks in the fingerprint region, including the peaks at 1358 and 1342 cm^{-1}, changed. The 1358 cm^{-1} peak decreased in intensity for all molecular weights, with the highest molecular weights showing the largest changes (Figure 4b); however, no clear dependence on the different annealing conditions was observed.

In solution, the relative intensities of the 1545 and 1608 cm^{-1} peaks changed very slightly as compared to thin films, preventing a direct comparison of the normalized peak intensities (I_{1358}/I_{1545}) between solution and thin film samples (Figure 4b). It is clear from Figure 4b, however, that there is no change in the I_{1358}/I_{1545} ratio in concentrated solutions over the entire molecular weight range investigated.

The significant changes in the vibrational mode intensities in solution and thin films may indicate changes in molecular conformation, ranging from isotropic solutions to polycrystalline annealed thin films. To understand the possible nature of these intensity changes, the vibrational transitions of an F8−BT−F8 oligomer were calculated in the infrared range with MOPAC using AM1 parameters. The calculated vibrational spectrum showed three transitions in the range between 1340 and 1360 cm^{-1} (Figure 4c). The peaks at 1342 and 1347 cm^{-1} were due to C−C and some C−H stretches mostly within the F8 unit. The peak at 1356 cm^{-1} contained a very strong contribution from the C−C stretch involving the two carbon atoms common to both the benzene ring and the thiadiazole unit in BT, a stretch that was found in no other transition. The intensity of this peak increased as the torsion angle between the F8 and BT units increased due to increased steric freedom (Figure 4c,d). This transition is, however, not strongly coupled to the fundamental electronic excitations as there are no significant changes in the absorption spectra for the pristine films as a function of molecular weight. The peaks at 1342 and 1347 cm^{-1} also showed some dependence on the torsion angle; however, systematic changes were not predicted.

The Raman data described above can thus be used to elucidate possible structural changes within these films. According to the calculated vibrational spectra, an increase in the 1358 cm^{-1} peak intensity would indicate a higher torsion angle between the F8 and BT units. (Note: The calculations were performed in the gas phase, and thus an absolute torsion angle cannot be extracted from the solid-state experimental data. For example, although

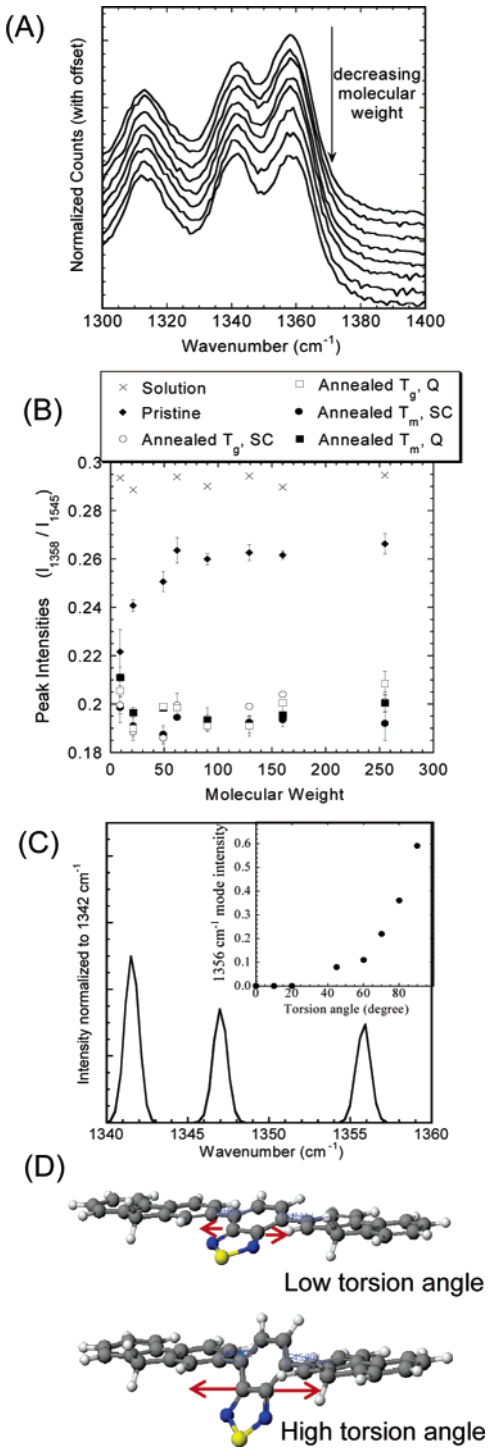

Figure 4. (A) Raman spectra of pristine films show a decrease in the intensity of the peak at 1358 cm^{-1} for the lowest few molecular weight F8BT molecules. Spectra have been offset for clarity. (B) Peak intensities of the 1358 cm^{-1} peak normalized to the 1545 cm^{-1} peak (I_{1358}/I_{1545}) for concentrated solutions (1.0−1.8% w/v), pristine films, and annealed films. (C) Calculated vibrational spectra in the range of 1340−1360 cm^{-1} for an F8−BT−F8 oligomer (neglecting the two $-C_8H_{17}$ side chains on each F8 unit) as a function of the torsion angle between the F8 and the BT planes. The data were calculated with MOPAC using AM1 parameters. A systematic decrease in the intensity of the 1358 cm^{-1} peak was observed as the torsion angle decreases (inset), indicating that annealed films (and low molecular weight pristine films) have a lower torsion angle than high molecular weight pristine films as shown in (B). (D) Illustrations of an F8−BT−F8 oligomer with a low (top) and high (bottom) torsion angle. The arrows indicate the carbon atoms in the BT unit involved in the C−C stretch and also the strength of the transition.

(24) McCreery, R. L. *Raman Spectroscopy for Chemical Analysis*; Wiley-Interscience: New York, 2000; Vol. 157.
(25) Kim, J.-S.; Ho, P. K. H.; Murphy, C. E.; Baynes, N.; Friend, R. H. *Adv. Mater.* **2002**, *14*, 206.
(26) Ariu, M.; Lidzey, D. G.; Bradley, D. D. C. *Synth. Met.* **2000**, *111−112*, 607.

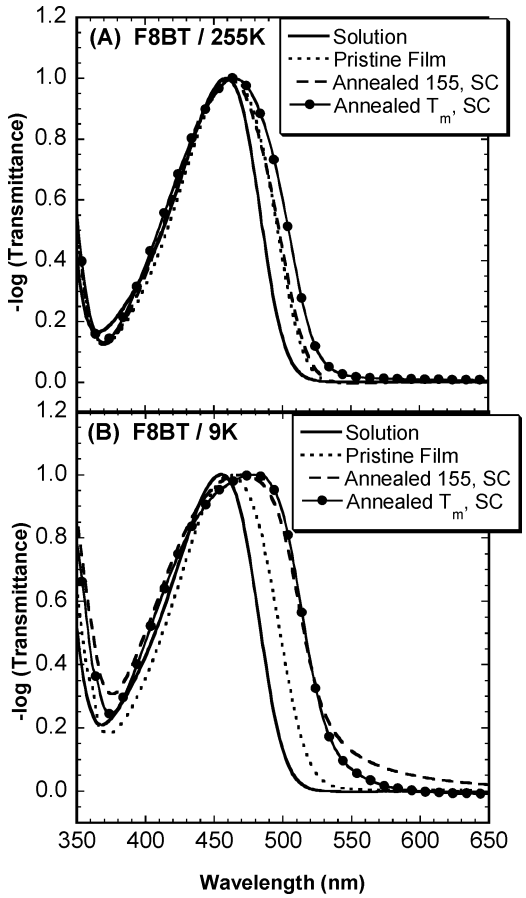

Figure 5. Normalized UV−visible absorption spectra of solutions (6×10^{-4}%, w/v), pristine films, and annealed films for (A) F8BT/255K and (B) F8BT/9K illustrating the broadening of the absorption peak upon film formation and annealing. The higher background at longer wavelengths for the film annealed to 155 °C in (B) is due to an increase in scattering effects because of the high surface roughness of this film.

the 1358 cm^{-1} peak is only observed at torsion angles $\geq 45°$ in the gas phase, this peak may be observed at much lower angles in the vibrational spectra of thin films.) The Raman data presented here suggest that the torsion angle in solutions is relatively high, but constant for all molecular weights, and is most similar to that observed in high molecular weight pristine films. Pristine films of low molecular weight F8BT seem to exhibit a smaller torsion angle, and the torsion angle decreases further for all molecular weights upon annealing, with the highest molecular weights showing the lowest torsion angles in annealed films.

UV−Visible Absorption. Absorption spectra of dilute solutions (6×10^{-4}%, w/v) show a blue shift of approximately 5 nm in the first absorption band appearing at ~460 nm as the molecular weight decreases (data not shown). Most of the observed shift occurred in F8BT/9K and F8BT/21K, corresponding to average degrees of polymerization of 5.7 and 13.4, similar to the effective conjugation length measured in PPV of ~10 monomer units.[27,28] This blue shift is even smaller in pristine thin films.

A comparison of dilute solution, pristine films, and annealed films is shown in Figure 5 for F8BT/255K and F8BT/9K. For both polymers, a similar broadening of the first absorption band toward longer wavelengths is observed upon film formation and annealing, although significantly more broadening is observed in the smaller polymer chains. The long and short polymer chains also display different temperature responses. Long chains only exhibit a broadening upon annealing to above T_m, while the short chains showed broadening for both annealing temperatures.

Photoluminescence (PL). PL spectra of dilute solutions (1.25×10^{-3}%, w/v) showed no significant differences between the different molecular weights. Pristine films showed a red shift compared to the spectra in solution[29] and exhibited at least two main emission states at 550 and 580 nm (Figures 6a,b for F8BT/255K and F8BT/9K, respectively). These two peaks were previously determined to be separate emissive states through a selective quenching of the low energy state by a PEDOT:PSS quenching interface.[30] There is a gradual shift in the relative intensities of these two components, with the higher energy component becoming more intense as the molecular weight decreased. Upon annealing, the high energy component becomes more intense for all of the samples.

For most conjugated polymer films, annealing has the effect of reducing the separation between the polymer backbones and increasing the likelihood of interchain states, such as aggregates in the ground state and excimers in excited states,[29,31,32] which typically show red-shifted, long-lived emission. Upon annealing F8BT films, however, emission preferentially occurs from the higher energy state. The emissive states do not show a shift to the red, as expected from the red-shifted absorption spectrum, indicating that while annealing may result in the formation of new low energy states, these states may be completely nonemissive. A similar blue shift upon annealing was recently observed in the emission of some poly(*p*-phenylenevinylene) derivatives.[33,34] This was attributed to a change in the polymer chain packing, but no specific model or change in packing was proposed.

PL efficiencies were measured on pristine and annealed films of these F8BT samples, and the results are shown in Figure 6c. In pristine films, PL efficiencies increase by approximately 5−10% as molecular weights increase. After annealing, the PL efficiencies of all samples increase by up to 10%. One sample (F8BT/62K), which shows a significantly lower PL efficiency as a pristine film, is known to contain a small amount of an inorganic impurity, as determined by inductively coupled plasma atomic absorption, and this impurity clearly affects the PL efficiency. After annealing, the impurity does not seem to affect the PL efficiency. These data have been included to illustrate the effect that impurities may play on the luminescence properties of conjugated polymers.

Changes in Charge Transport (Electron Mobilities). N-type transistors were fabricated with the structure shown in Figure 7a. The use of a BCB dielectric layer has been shown

(27) Tian, B.; Zerbi, G.; Schenk, R.; Mullen, K. *J. Chem. Phys.* **1991**, *95*, 3191.
(28) Tian, B.; Zerbi, G.; Mullen, K. *J. Chem. Phys.* **1991**, *95*, 3198.
(29) Nguyen, T.-Q.; Martini, I. B.; Liu, J.; Schwartz, B. J. *J. Phys. Chem. B* **2000**, *104*, 237.
(30) Kim, J.-S.; Grizzi, I.; Burroughes, J. H.; Friend, R. H. *Appl. Phys. Lett.* **2005**, *87*, 023506.
(31) Nguyen, T.-Q.; Kwong, R. C.; Thompson, M. E.; Schwartz, B. J. *Appl. Phys. Lett.* **2000**, *76*, 2454.
(32) Ruseckas, A.; Namdas, E. B.; Ganguly, T.; Theander, M.; Svensson, M.; Andersson, M. R.; Inganas, O.; Sundstrom, V. *J. Phys. Chem. B* **2001**, *105*, 7624.
(33) Mikroyannidis, J. A.; Spiliopoulos, I. K.; Kasimis, T. S.; Kulkarni, A. P.; Jenekhe, S. A. *Macromolecules* **2003**, *36*, 9295.
(34) Mikroyannidis, J. A.; Vellis, P. D.; Karastatiris, P. I.; Spiliopoulos, I. K. *Synth. Met.* **2004**, *145*, 87.

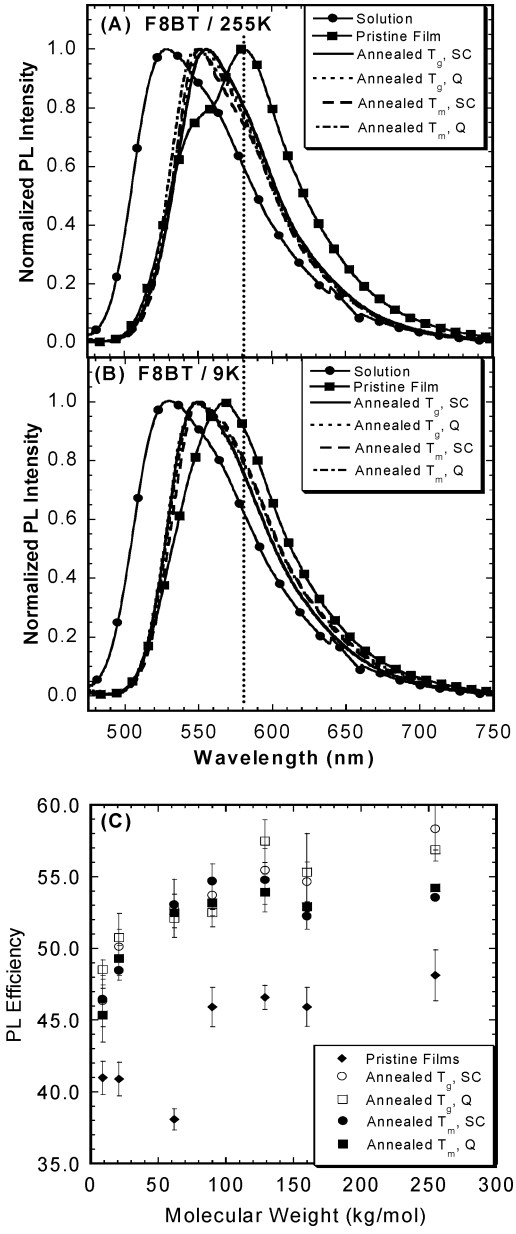

Figure 6. Photoluminescence spectra of solutions (1.25×10^{-3}%, w/v), pristine films, and annealed films for (A) F8BT/255K and (B) F8BT/9K, all obtained in an integrating sphere. The dotted vertical line allows a comparison of the energies of the PL peaks in pristine films. (C) PL efficiencies for pristine and annealed films. The sample with a molecular weight of 62 kg/mol is known to have some inorganic impurities and shows a low PL efficiency.

to enable the observation of clean electron transport in polymer semiconductors by avoiding charge trapping of electrons at the interface.[17,18] Raman data of F8BT pristine and annealed films on BCB showed that the 1358 cm^{-1} peak intensities were similar to those observed without the BCB layer, and the same general trends were also observed for the different molecular weights and annealing conditions. In addition, WAXS data have confirmed the same crystalline structure is obtained in F8BT/255K films annealed to T_m on silicon and on BCB. All F8BT films used in a transistor structure were annealed to at least 100 °C, a temperature lower than the T_g, but high enough to remove any solvent trapped in the film. Films that were only annealed to this temperature will be referred to as "pristine" to denote that they have been processed only slightly differently

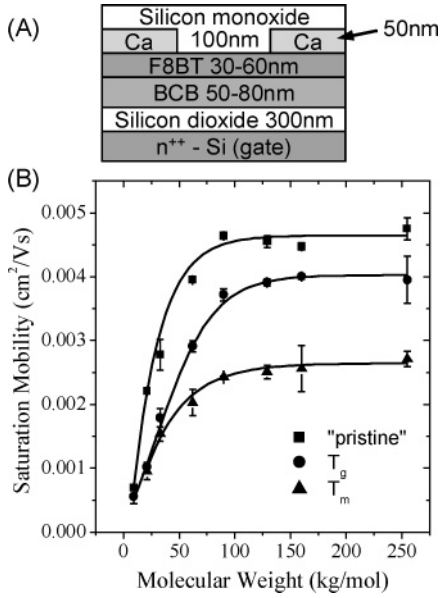

Figure 7. (A) Schematic illustration of the n-type F8BT transistor fabricated for this study. (B) Electron mobilities calculated in the saturation region for F8BT films annealed to different temperatures. Decreases in mobility were observed upon annealing and for the shorter molecular weights. "Pristine" films are those that were heated only to 100 °C to remove residual solvent trapped in the films before further processing steps.

than the pristine films used in previous experiments; we consider the packing structure in these films to be similar to that in the pristine films described earlier. Mobilities were measured in the saturation region, and a plot of mobility as a function of molecular weight is shown in Figure 7b. Electron mobilities ranged from 6×10^{-4} to 4.8×10^{-3} $cm^2/V \cdot s$ and were highest for "pristine" high molecular weight films. Mobilities decreased as the molecular weight decreased and also as the films were annealed to above the T_g and above the T_m of the material. These mobilities are similar to those measured in a time-of-flight experiment;[35] however, differences such as electric field, film thickness, and the geometry of the experiment with respect to the orientation of the molecules prevent a direct comparison between the two experiments.

Previous studies have illustrated the importance of molecular orientation on the charge carrier mobility measured in a transistor structure.[20] Intrachain electron transport in F8BT is not expected to be a very efficient process, due to the strong localization of electrons in the LUMO on the BT units and the high energy barrier that the F8 sites would present as an electron moved along the chain.[12] Thus, charge transport in F8BT is thought to be dominated by interchain hopping events along the π-stacking direction, and therefore, the ideal molecular orientation would be that shown in Figure 2h. We have shown, however, that the predominant structure in annealed films of F8BT is represented by Figure 2g. Surprisingly, the electron mobilities in these samples are still relatively high ($\sim 2.5 \times 10^{-3}$ $cm^2/V \cdot s$), indicating that a significant amount of electron transport occurs either along the polymer chain (BT spacing of $\sim$14.65 Å, making this unlikely) or due to hopping events from chain to chain, in a direction parallel to the substrate in Figure 2g. The unit cell spacing in this direction according to the WAXS data is rather small (chain-to-chain spacing = 5.3 Å,

(35) Cambell, A. J.; Bradley, D. D. C.; Antoniadis, H. *Appl. Phy. Lett.* **2001**, *79*, 2133.

Table 2. Summary of Experimental Results

technique	effect of annealing	effect of decreasing MW
WAXS	induce ordered crystalline domains (except for F8BT/9K T_m)	more isotropic orientation of the π-stacking multiple unit cells observed upon annealing
AFM	increase in surface RMS roughness	increase in surface RMS roughness unique morphology in F8BT/9K T_g
Raman	increase in planarity	increase in planarity
UV/visible absorption	the first absorption band broadens to lower energies	the first absorption band shows small shift to lower energies
PL spectra	high energy component becomes more intense	high energy component becomes more intense
PL efficiencies	increase in PL efficiency	decrease in PL efficiency
electron mobility	decrease in mobility	decrease in mobility

BT−BT interchain spacing depends on the in-plane packing geometries, but is less than the intrachain BT spacing of 14.65 Å) and may explain why these mobilities are approximately an order of magnitude higher than those measured in a similar direction in some polythiophene films, where this spacing is much larger (16.5 Å).[20] Current efforts to align F8BT molecules will allow us to measure mobilities in the two in-plane directions and determine the major pathway for electron transport.

Discussion

Proposed Structural Model for F8BT Packing Structure. The results described above are summarized in Table 2, and they indicate that considerable changes occur within F8BT polymer thin films as a function of molecular weight and annealing. On the basis of the results presented above and previously published quantum calculations of F8BT,[12] a model was developed to explain the changes in these films as a function of molecular weight and annealing.

The lowest energy configuration of a single F8−BT−F8 oligomer in the ground state was determined in the gas phase through modeling studies (MOPAC-AM1), and in this configuration, the conjugated planes of the F8 and BT units are twisted with respect to one another by 45° for steric reasons. (Note: In this calculation, the alkyl chains were omitted for simplicity. These chains are not expected to greatly affect the torsion angle between the F8 and BT units in the gas phase or the electronic properties of the molecule; however, they will affect the three-dimensional packing structure of the polymers in thin films. The alkyl chains were not included in our model since they are present for all of the molecules described; however, we do acknowledge their importance in the solid-state packing.)

In solution, the polymers are expected to retain a significant torsion angle between these two units, which will likely be exhibited to some extent in pristine spin-coated films, as demonstrated by Raman spectroscopy. Figure 8a illustrates the polymer packing geometry thought to dominate pristine thin films for the high molecular weight polymers. During the relatively fast spin-coating process, the polymer chains do not have enough time to find an ideal low energy packing geometry, and because of the relatively high torsion angle between the F8 and BT units, neighboring polymers may adopt a packing structure similar to that shown in Figure 8a, where the BT units in neighboring chains are adjacent to one another to minimize steric hindrances. The schematic in Figure 8a is a highly idealized illustration of the packing in these pristine films, and a significant portion of the film is thought to be relatively

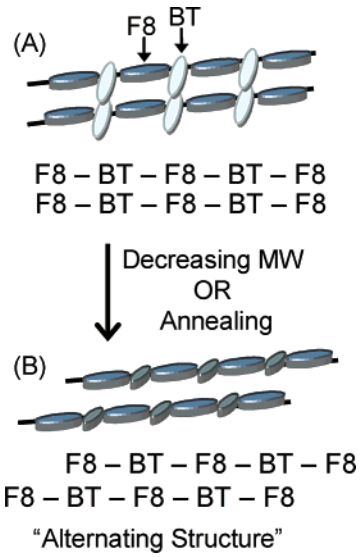

Figure 8. Schematic illustrations showing (A) the initial packing structure of the high molecular weight pristine films. The BT units exhibit a relatively high torsion angle with respect to the F8 units, and in neighboring polymer chains, the BT units are adjacent to each other. (B) The packing structure for the low molecular weight pristine films or annealed films. Adjacent polymer chains have been translated with respect to one another, so that the BT units in one chain are adjacent to the F8 units in the neighboring chain (termed "alternating structure"). This structure forces the BT units into a geometry that is more planar with the F8 units.

disordered, as indicated by the WAXS scattering pattern in Figure 2a. Even so, the pristine films are thought to have more BT units in neighboring chains adjacent to one another than the annealed films. In addition, the orientation of the BT units most likely will not be as ordered as illustrated. In fact, the dipole on the BT unit will force the BT units to alternate both their direction and their torsion angles (positive or negative torsion angle) in macroscale polymer packing, so that the dipoles cancel one another. The proximity of the dipoles on the BT units in this geometry should still render this packing geometry relatively high in energy.

If the polymer chains are able to arrange themselves in a more energetically favorable structure, either with relatively mobile short chains or through annealing, we expect the BT units in neighboring chains to repel one another. In this configuration, the BT units would occupy positions adjacent to F8 units in the neighboring polymer chains (alternating structure, Figure 8b). To shift one F8BT chain by half a repeat unit with respect to its neighbor, the BT unit is required to adopt a more planar orientation with respect to the F8 units (as described by the

Raman data). This new packing structure allows less overlap between BT units in neighboring chains, exhibits a smaller torsion angle, and is more crystalline than the structure in Figure 8a. We will discuss how the changes observed in the optical and charge transport properties described above can be accounted for by this proposed model.

Optical Effects. The broadening of the UV/visible absorption peak to longer wavelengths upon film formation and annealing could indicate the formation of a new low energy state due to interchain aggregate states between polymer chains. Wide-angle X-ray scattering (WAXS) experiments, however, did not show a change in the π-stacking spacing between polymer chains; a decrease in this spacing is expected to increase the likelihood of aggregate formation. Even with a constant spacing in the π-stacking direction, it may be possible for changes in the packing structure to induce the formation of aggregate states. The interaction between two polymer chains in the ground state may be much stronger in the alternating structure adopted after annealing than in the more random configuration before annealing, and may lead to the formation of lower energy aggregate states. An extension of the effective conjugation length due to a more planar conjugated polymer backbone may also be responsible for the new low energy state observed. Calculations based on an F8−BT−F8 oligomer (calculated with ZINDO at the INDO/SCI level) have shown that decreasing the torsion angle between the F8 and BT units will increase the planarity of the polymer backbone and thus the effective conjugation length, thereby causing the first absorption band to shift to longer wavelengths.

The exact nature of the emissive states in F8BT is not well-known; however, the changes in relative intensities of the two main PL components observed here indicate the existence of multiple electronic states and the possible energy transfer between these states.[30] Cornil and co-workers have calculated the optical coupling, which is proportional to the rate of exciton transfer between two neighboring chains, for F8BT as a function of the translation of one F8BT chain with respect to its neighboring chain.[12] It is found that the strong localization of the electron on the BT unit in the LUMO restricts the movement of both electrons and excitons to the BT units and results in interchain energy transfer that is significantly more likely when BT units in neighboring chains are adjacent to one another. The emission from low energy states in pristine high molecular weight films (Figure 8a) may, therefore, be the result of efficient energy transfer to this state from the higher energy state due to a favorable arrangement of BT units in neighboring chains.

Efficient energy transfer is usually associated with low PL efficiencies due to the migration of excitons to low energy states that are often nonemissive or weakly emissive.[31,32,36] After annealing, the PL efficiencies of all samples increase, consistent with the idea that the polymer chains are arranged in such a way that energy transfer to lower energy, nonemissive sites is less efficient (BT units in adjacent chains are relatively far apart, Figure 8b).

In pristine films, PL efficiencies increase by approximately 5−10% as molecular weights increase, in contrast to that predicted by the model in Figure 8. The model predicts that the high molecular weight samples should show the most efficient energy transfer and thus the lowest PL efficiencies. It is possible that another effect is competing in the low molecular weight films with the effects predicted by the model proposed. For example, the percentage of excitons formed near chain ends would be much larger than for the higher molecular weight samples. If chain ends act as exciton dissociation sites, PL efficiencies would decrease with decreasing molecular weight. This effect may be much stronger than the differences in energy transfer efficiencies due to polymer packing structure, resulting in lower PL efficiencies for the low molecular weight samples.

Charge Transport. In pristine films, there are a number of possible reasons why electron mobilities may increase as a function of increasing molecular weight.[37] These possibilities include (i) chain ends acting as trap sites, (ii) the distance a charge can travel before it is required to hop to another polymer chain, (iii) low-lying trap states due to high polydispersities or incomplete sample crystallization, and (iv) morphology and/or packing structure of the polymer chains. These possibilities are addressed below.

Low molecular weight samples will contain more chain ends than higher molecular weight samples, and these chain ends may act as chemical trap sites for electrons. The F8BT samples described above have all been end-capped with benzene rings to prevent chemical traps at the end of the chain. Recent results have shown, however, that even when this end-capping is not performed, and the chain ends are terminated with bromine atoms, there is no significant difference in mobilities as compared to the end-capped samples of similar molecular weight. These results are similar to those obtained by Kline and co-workers,[37] although in our work, some differences in threshold voltages were also observed. Thus, it is unlikely that the chain ends act as a chemical trap for electrons in the sample.

It is commonly thought that in conjugated polymers, charge transport is most efficient along a single chain, and that charges will prefer to stay within that chain until they are forced to hop to another. Thus, chain ends can also act as physical traps, requiring more frequent interchain hopping events for the shorter polymer chains. If electron transport in F8BT is indeed dominated by interchain hoping events as discussed earlier, then the differences in the number of chain ends in films of different molecular weights will not significantly influence the measured electron mobilities. In addition, this argument would not explain the different mobilities measured in films annealed to different transition temperatures.

Recently, it has been demonstrated that in samples with high polydispersities, polymer chains that are significantly longer than the average chain length can present low energy states that can act as trap sites.[38] Low energy trap states may also result from samples that are incompletely crystallized and present energetic disorder in the sample. The lower molecular weight samples in this study do exhibit larger polydispersities (Table 1); however, the threshold voltages in pristine films did not show a significant increase as the polydispersities increased. In addition, annealing actually seemed to decrease threshold voltages slightly, indicating that the reduced mobilities were not the result of low energy trap states. Absorption data showed no significant change in

(36) Harrison, M. G.; Friend, R. H. Optical Applications. In *Electronic Materials: The Oligomer Approach*; Mullen, K., Wegner, G., Eds.; Wiley-VCH: Weinheim, Germany, 1998; p 515.

(37) Kline, R. J.; McGehee, M. D.; Kadnikova, E. N.; Liu, J.; Frechet, J. M. J. *Adv. Mater.* **2003**, *15*, 1519.

(38) Menon, A.; Dong, H.; Niazimbetova, Z. I.; Rothberg, L. J.; Galvin, M. E. *Chem. Mater.* **2002**, *14*, 3668.

the band gap for the range of pristine polymers studied here (pristine thin films show a shift that is less than 5 nm). PL spectra, which are more sensitive to small populations of low energy trap sites due to the energetic relaxation that occurs to low energy sites before emission, actually show a shift to higher energies upon annealing. Thus, the presence of low-lying trap states can be safely ruled out.

Finally, the effect of film morphology and polymer packing structure must be addressed. There is significant evidence for differences in polymer packing geometries in pristine films and further restructuring in annealed F8BT films, which may affect the efficiency of electron transport. As discussed earlier, intrachain electron mobilities are expected to be relatively low, and therefore, the movement of electrons in an F8BT film may depend more strongly on interchain transport and the specific arrangement of the polymers within the unit cell. Cornil and co-workers calculated that the electronic coupling (and therefore electron mobilities) would be higher when BT units in neighboring chains were adjacent to one another (Figure 8a).[12] This is the case in our "pristine" films of high molecular weights. As the molecular weight decreases or the films are annealed, a reorganization of the polymer chains into the "alternating structure" forces the BT units in neighboring chains further apart (Figure 8b) and makes interchain electron transport less efficient, resulting in decreased electron mobilities.

Conclusions

Our studies of F8BT spin-coated films of different molecular weights upon annealing have indicated a restructuring of the packing structure which affects both the optoelectronic and charge transport properties of these films. In pristine films, there is evidence for a significant torsion angle between the F8 and BT units, and a large number of BT units in neighboring chains are adjacent to one another. The local dipole in the BT unit in F8BT dictates a low energy packing geometry in which the BT units in one polymer chain are adjacent to the F8 units in the neighboring chain. Upon annealing to a sufficiently high temperature, this "alternating" packing structure is achieved, allowing the BT units in adjacent chains to move away from one another.

Due to the localized nature of the electron in the LUMO of F8BT, energy transfer and electron transfer become more difficult as the BT units in neighboring chains are separated from one another. Thus, after annealing, the PL spectrum exhibits more emission from a high energy state (less energy transfer to lower energy less emissive states), and PL efficiencies increase concurrently. In addition, electron mobilities decrease after annealing because the BT units are relatively far apart, their wave function overlap is reduced, and interchain electron transport becomes more difficult. These results are in many ways very different from reports on other conjugated polymers upon annealing;[29,31,36] however, the strong charge localization observed in F8BT is rather unique, and it is thought to be responsible for the differences observed.

Acknowledgment. The authors would like to thank CDT for the F8BT materials studied here, I. Grizzi and C. Foden for helpful discussions, A. Goodsell and P. Montes for assistance with solution PL and DSC measurements, J. Cornil for valuable comments, and J. M. Winfield for taking the ellipsometry data. J.S.K. thanks the EPSRC for an Advanced Research Fellowship.

JA051891J